Subnitride chemistry: A first-principles study of the $NaBa_3N$, Na_5Ba_3N, and $Na_{16}Ba_6N$ phases

Josep M. Oliva*

Instituto de Química-Física "Rocasolano", CSIC, Serrano 119, E-28006 Madrid, Spain

Abstract

An ab initio study on the electronic structure of the subnitrides $NaBa_3N$, Na_5Ba_3N, and $Na_{16}Ba_6N$ is performed for the first time. The $NaBa_3N$ and Na_5Ba_3N phases consist of infinite $^1_\infty[NBa_{6/2}]$ strands composed of face-sharing NBa_6 octahedra surrounded by a "sea" of sodium atoms. The $Na_{16}Ba_6N$ phase consist of discrete $[NBa_6]$ octahedra arranged in a body-cubic fashion, surrounded by a "sea" of sodium atoms. Our calculations suggest that the title subnitrides are metals. Analysis of the electronic structure shows partial interaction of $N(2s)$ with $Ba(5p)$ electrons in the lower energy region for $NaBa_3N$ and Na_5Ba_3N. However, no dispersion is observed for the $N(2s)$ and $Ba(5p)$ bands in the cubic phase $Na_{16}Ba_6N$. The metallic band below the Fermi level shows a strong mixing of $N(2p)$, $Ba(6s)$, $Ba(5d)$, $Ba(6p)$, $Na(3s)$ and $Na(3p)$ orbitals. The metallic character in these nitrides stems from delocalized electrons corresponding to hybridized $5d^l6s^m6p^n$ barium orbitals which interact with hybridized $3s^n3p^m$ sodium orbitals. Analysis of the electron density and electronic structure in these nitrides shows two different regions: a metallic matrix corresponding to the sodium atoms and the regions around them and heteropolar bonding between nitrogen and barium within the infinite $^1_\infty[NBa_{6/2}]$ strands of the $NaBa_3N$ and Na_5Ba_3N phases, and within the isolated $[NBa_6]$ octahedra of the $Na_{16}Ba_6N$ phase. The nitrogen atoms inside the strands and octahedra are negatively charged, the anionic character of nitrogens being larger in the isolated octahedra of the cubic phase $Na_{16}Ba_6N$, due to the lack of electron delocalization along one direction as opposed to the other phases. The sodium and barium atoms appear to be slightly negatively and positively charged, the latter to a larger extent. From the computed Ba–N overlap populations as well as the analysis of the contour maps of differences between total density and superposition of atomic densities, we suggest partial covalent bonding between nitrogen and barium atoms along the infinite $^1_\infty[NBa_{6/2}]$ strands and within isolated $[NBa_6]$ octahedra.

1. Introduction

Subnitride chemistry provides an interesting area of new materials with unusual physical and chemical properties. From the physical point of view, alkaline and alkaline-earth subnitrides [1] have interesting properties such as low electronic work function, due to the quantum confinement of the conduction electrons [2]. From the chemical point of view, the bonding in these compounds is remarkable, as recently proposed by

Röhr [3] and Simon and co-workers [4–6]. These authors propose an interstitial metallic region with Na–Ba metallic bonding, separating zero-dimensional isolated $[NBa_6]$ octahedra or one-dimensional infinite $^1_\infty[NBa_{6/2}]$ strands featuring Ba–N ionic bonding.

The recently discovered sodium–barium nitrides have structural analogies with the already known rubidium and cesium suboxides, discovered almost a hundred years ago and structurally characterized in the late 1970s by Simon and co-workers [7].

The subnitrides studied in this work, $NaBa_3N$, Na_5Ba_3N and $Na_{16}Ba_6N$, appear as impurities in sodium rich liquid alloys of sodium–barium, which

*Fax: + 34 91 5642431.

E-mail address:* J.M.Oliva@iqfr.csic.es.

absorb nitrogen gas readily. The barium subnitrides can be classified according to the arrangement of the inverse clusters through the ratio A/X, where A is the number of corners of the NBa_6 octahedra and X the number of centers of octahedra (see Table 1 and Fig. 1 of Ref. [3]). Thus, $A/X = 3$ for the $NaBa_3N$ and Na_5Ba_3N phases, and $A/X = 6$ for the $Na_{16}Ba_6N$ phase. There also exist subnitride phases with other values of A/X, such as the complex phase $Na_{14}Ba_{14}CaN_6$ with $A/X = 2.5$ [8,9].

The goal of this work is to carry out a comprehensive study of the electronic structure of the recently discovered barium subnitrides $NaBa_3N$, Na_5Ba_3N, and $Na_{16}Ba_6N$, by means of first-principles density-functional theory (DFT) methods. The manuscript is organized as follows: Section 2 includes the computational approach used in the electronic structure calcula-

tions; Section 3 discusses the electronic structure of the title compounds: band structure, density of states and bonding. Finally Section 4 provides the conclusions reached.

2. Computational details

All calculations in this work were performed with the recently developed SIESTA code [10], which makes use of the DFT [11,12] with numerical local bases. We used the generalized gradient approximation (GGA) of the exchange-correlation potential of DFT due to Perdew et al. [13]. The "active" space in the calculations corresponds to the valence electrons, while the core or "inactive" electrons are substituted by suitable norm-conserving scalar pseudopotentials [14] (a relativistic pseudopotential was used for barium) factorized in the Kleinman–Bylander form [15]. The pseudopotentials were generated with the following atomic configurations (active/valence electrons are indicated outside the square brackets) and core cutoff radii, respectively: Nitrogen $\rightarrow [He]2s^2 2p^3$ and 1.25 a.u. for all components; Sodium $\rightarrow [Ne]3s^{0.3}$ and 3.50 a.u., 4.00 a.u., and 3.50 a.u. for the s, p and d components, respectively; Barium $\rightarrow [[Kr]4d^{10}5s^2]5p^6 6s^2$, and 1.90 a.u., 3.80 a.u., and 2.80 a.u. for the s, p and d components, respectively. The integrals involved in the Kohn–Sham Hamiltonian are computed using a regular real space grid where the electron density is projected. The Hartree potential is computed using fast Fourier transforms in that grid. The grid spacing is determined by the maximum kinetic energy of the plane waves that can be represented in that grid. In this work we used a cutoff of 400, 100 and 100 Ry for the $NaBa_3N$, Na_5Ba_3N, and $Na_{16}Ba_6N$ phases, respectively, which corresponds to a grid spacing of 0.085, 0.165 and 0.165 Å, respectively. The Brillouin zone (BZ) was sampled with an $8 \times 8 \times 8$, $5 \times 5 \times 5$, and $4 \times 4 \times 4$ Monkhorst–Pack grid, respectively for $NaBa_3N$, Na_5Ba_3N, and $Na_{16}Ba_6N$, the total number of k-points used in the irreducible part of the BZ being 320, 75 and 48, respectively. A linear combination of numerical pseudo-atomic orbitals (PAOs) with a finite range r_c are used as basis functions [16]. The shape of the different orbitals is obtained by imposing that the wave function vanishes at given confinement radii r_c, which are determined by the *energy shift*, namely the energy increase of the atomic eigenstate due to the confinement. In this work we used energy shifts of 500, 500, and 250 meV for the $NaBa_3N$, Na_5Ba_3N, and $Na_{16}Ba_6N$ phases, respectively. The confined basis sets used in the calculations are split-valence, in the same context as in quantum chemistry [17,18]. The polarization orbitals are obtained by computing the response of the occupied orbital to an external electric field. A systematic study of the basis set in the $NaBa_3N$ phase showed that a single-ζ basis with an additional set of $5d$

Table 1
Mulliken charges (in units of $|e|$) in the $NaBa_3N$, Na_5Ba_3N, and $Na_{16}Ba_6N$ phases

	$NaBa_3N$	Na_5Ba_3N	$Na_{16}Ba_6N$
Na(1)	−0.197	−0.073	−0.055
Na(2)	—	−0.049	0.007
Na(3)	—	−0.058	—
Na(4)	—	−0.002	—
Ba(1)	0.142	0.151	0.099
Ba(2)	—	0.110	—
Ba(3)	—	0.151	—
N	−0.228	−0.228	−0.455

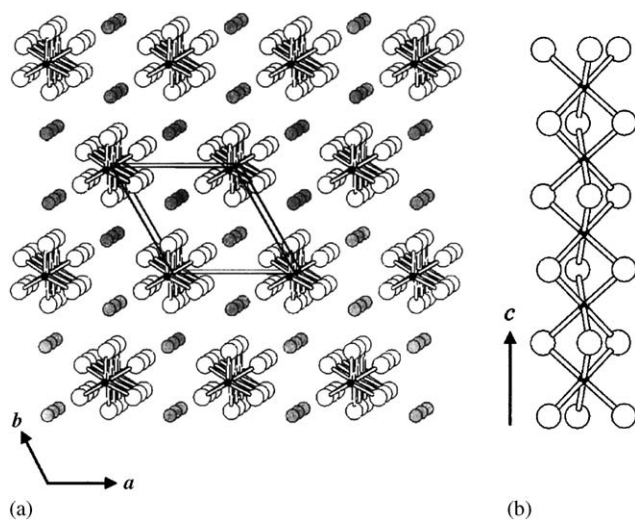Fig. 1. (a) Projection of the $NaBa_3N$ structure along c. The barium and nitrogen atoms are bound by lines showing the $^1_\infty[NBa_{6/2}]$ strand structures along c surrounded by sodium atoms. White, black and gray spheres correspond, respectively, to barium, nitrogen and sodium atoms. (b) One of the infinite $^1_\infty[NBa_{6/2}]$ strands of the $NaBa_3N$ phase along c. The face-sharing NBa_6 octahedra are perfect. White and black spheres correspond, respectively, to barium and sodium atoms.

functions on barium and a respective set of polarization $3p$ and $6p$ functions on sodium and barium, properly reproduces the band structure of $NaBa_3N$ with larger basis sets. We therefore used the same basis for the Na_5Ba_3N and $Na_{16}Ba_6N$ phases. For a more detailed description of the methodology used in this work, the reader is referred to Ref. [10]. All calculations were carried out with the atomic positions and lattice parameters from the experimental crystalline structures [4–6].

3. Electronic structure: results and discussion

Fig. 1a shows the crystal structure of the $NaBa_3N$ phase along the c-axis. The hexagonal structure consists of a close packing of sodium and barium atoms filled with nitrogen atoms. The barium and nitrogen atoms form infinite $^1_\infty[NBa_{6/2}]$ strands along c, composed of face-sharing perfect NBa_6 octahedra, with single sodium atoms arranged between these close-packed strands, as shown in Fig. 1b.

The crystal structure of the Na_5Ba_3N phase, projected along the b-axis is shown in Fig. 2. The infinite $^1_\infty[NBa_{6/2}]$ strands along the b-axis are very similar to those in the $NaBa_3N$ phase, but slightly distorted. Another difference is the presence of more sodium atoms in the interstitial areas between the $^1_\infty[NBa_{6/2}]$ rods, as compared to $NaBa_3N$. Therefore the structural simila-

rities of these two phases are the coordination of the barium and nitrogen atoms, forming an infinite strand along one of the crystallographic axes, the difference between them being the amount of sodium atoms between these strands.

The crystal structure of the $Na_{16}Ba_6N$ phase is shown in Fig. 3, where discrete perfect $[NBa_6]$ octahedra are arranged in a body-cubic fashion, surrounded by sodium atoms [6]. An isotypic phase of $Na_{16}Ba_6N$, containing discrete NCa_6 octahedra is the $Ag_{16}Ca_6N$ phase [19], previously known as Ag_8Ca_3 [20].

3.1. Band structure

Figs. 4a–c show, respectively, the BZ of the reciprocal lattice in the $NaBa_3N$ (hexagonal), Na_5Ba_3N (simple orthorhombic), and $Na_{16}Ba_6N$ (simple cubic) phases. Also shown in these figures are the high symmetry points of the BZ used in the analysis of the band structure. Figs. 4a–c show, respectively, the band structure of the $NaBa_3N$, Na_5Ba_3N, and $Na_{16}Ba_6N$ phases. The lower energy bands in all three phases can be divided into three regions: The first and third region (from bottom to top) both correspond to the $N(2s)$ electrons which interact with a fraction of the $Ba(5p)$ electrons (see also Fig. 5). As shown in Figs. 4a and b, the only directions which show dispersion in these regions are $A \to \Gamma$, $L \to M$, and $H \to K$ for $NaBa_3N$, and $S \to X$, $Y \to \Gamma$, $R \to U$, and $T \to Z$ for Na_5Ba_3N.
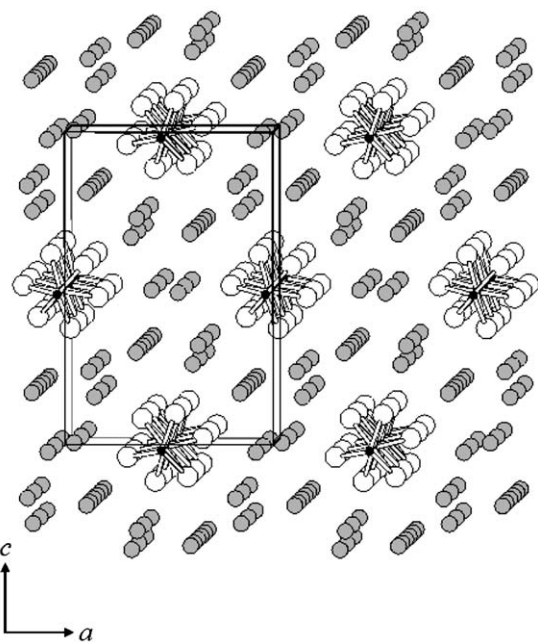

Fig. 2. Projection of the Na_5Ba_3N structure along b. The barium and nitrogen atoms are bound by lines showing the strand structures along c surrounded by sodium atoms. The infinite $^1_\infty[NBa_{6/2}]$ strands along b are similar to those in the $NaBa_3N$ but slightly distorted. White, black and gray spheres correspond, respectively, to barium, nitrogen and sodium atoms.
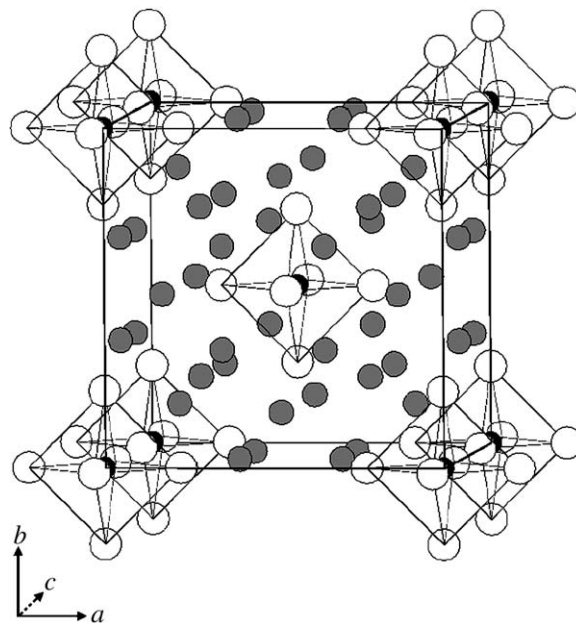

Fig. 3. Projection of the $Na_{16}Ba_6N$ structure along c. The perfect $[NBa_6]$ octahedra (shown in the figure) are arranged in a body-cubic fashion at the center and vertices of the cube and are surrounded by a "sea" of sodium atoms. No lines connecting barium and nitrogen in the octahedral are shown for clarity. White, black and gray spheres correspond, respectively, to barium, nitrogen and sodium atoms.
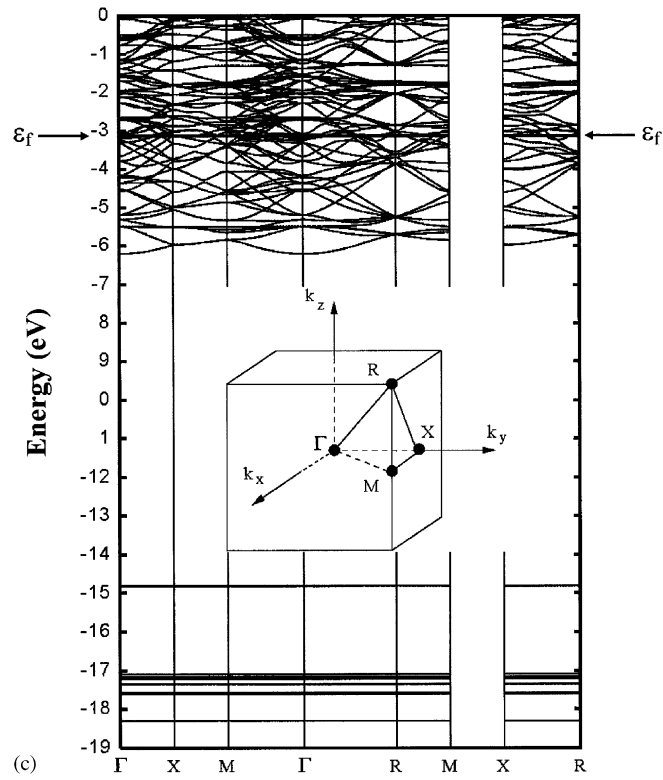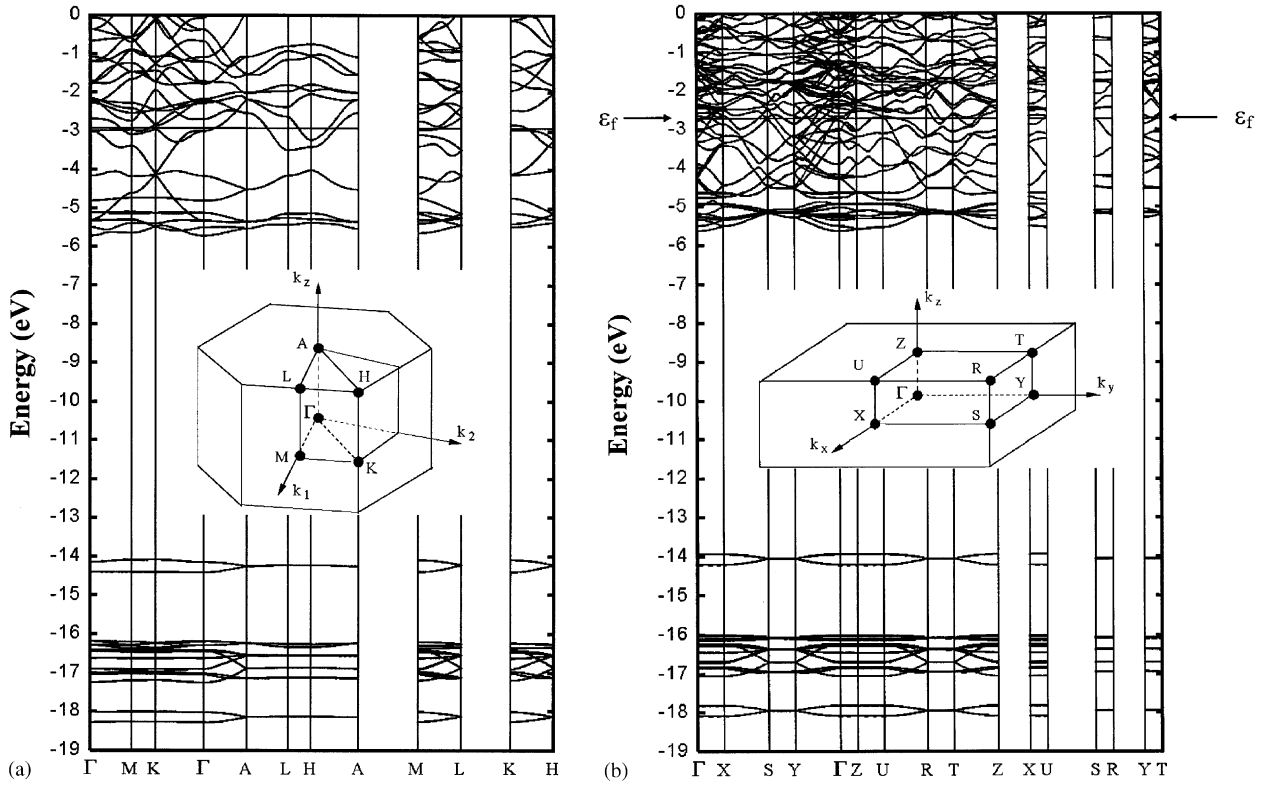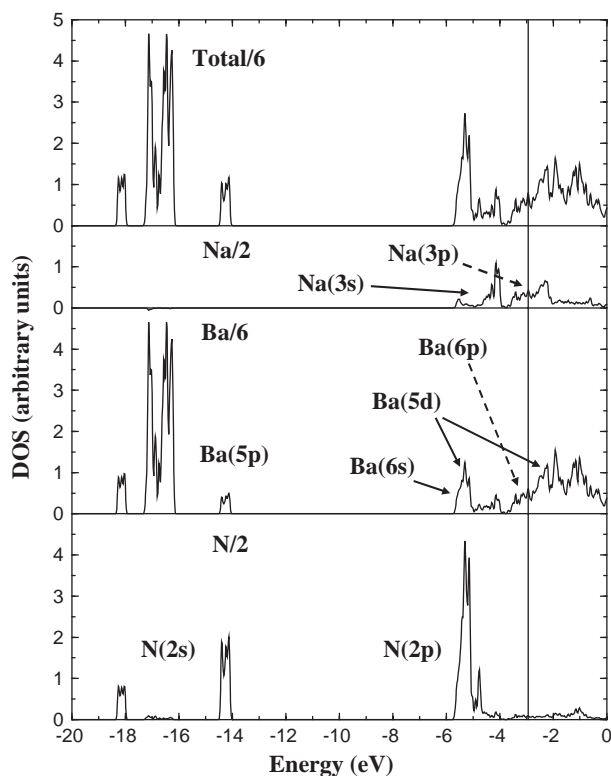
Fig. 5. Total and atom-projected density of states (DOS) in the NaBa$_3$N phase. The total, sodium-, barium- and nitrogen-projected DOS are divided, respectively, by six, two, six and two.

These directions in reciprocal space correspond, respectively, to z and y in real space for NaBa$_3$N and Na$_5$Ba$_3$N. In both nitrides these directions correspond to the axis of the infinite $^1_\infty$[NBa$_{6/2}$] tubes/strands. As regards to the cubic phase (Fig. 4c), no dispersion is shown in the three regions of the lower bands area whatsoever. Therefore the $N(2s)$ and Ba(5p) electrons hardly interact with one another in the cubic phase Na$_{16}$Ba$_6$N. The second (middle) region of the lower bands corresponds mainly to the Ba(5p) electrons. Dispersion is also shown in certain bands of this area along the same directions of the reciprocal space as mentioned above, corresponding to the real space direction of the infinite $^1_\infty$[NBa$_{6/2}$] strands.

Let us now turn to the metallic band around the Fermi level. Figs. 4a–c show appreciable band disper-

sion and crossing of bands around the Fermi level for all three phases and practically all high-symmetry directions of the reciprocal space. Therefore these three nitrides should be regarded as three-dimensional metals. Obviously, the increasing number of sodium and, to a less extent, barium atoms in the series NaBa$_3$N, Na$_5$Ba$_3$N, and Na$_{16}$Ba$_6$N provides a larger number of bands around the Fermi level.

3.2. Density of states

Fig. 5 depicts, respectively, the total and atom-project density of states (DOS) of the NaBa$_3$N phase (the DOS of the Na$_5$Ba$_3$N and Na$_{16}$Ba$_3$N phases have been also computed and show similar profiles). Due to the large number of atoms in these phases, the DOS are "normalized" in such a way that the unit of the DOS is similar for all atoms. Since we included the 5p^6 electrons of barium in the calculations, a big peak always appears in the DOS corresponding to these electrons. Therefore, our "normalization" of the DOS consists of dividing by Z (number of formula units per unit cell) and the number of barium atoms the total and atom-projected DOS, as shown in Fig. 5, as follows:

$$\text{normalised total/atom} - \text{projected DOS}$$
$$= \frac{\text{total/atom} - \text{projected DOS}}{Z \times N_{\text{Ba}}}.$$

Thus, in the Na$_{16}$Ba$_6$N phase, e.g., we have $Z = 4$ and therefore the total DOS is divided by $Z \times N_{\text{Ba}} = 24$, and the atom-projected DOS is divided by 64, 24, and four for sodium, barium, and nitrogen, respectively. Fig. 5 shows a strong mixing of N(2p), Ba(6s, 5d, 6p), and Na(3s, 3p) in the valence region below the Fermi level. However, the main contributions at the Fermi level in all three nitrides correspond to Ba(6s,5d,6p) and Na(3s,3p) states.

3.3. Bonding

Table 1 gathers the atomic Mulliken populations of the sodium, barium and nitrogen atoms of the three subnitrides. In NaBa$_3$N, the sodium atoms are fairly negatively charged, as compared to the other phases. However, in Na$_5$Ba$_3$N, the sum of the charges of the

Fig. 4. (a) Band structure of the NaBa$_3$N phase from the lowest energy bands to the valence bands near the Fermi level ε_F (straight solid line). Shown as inset is the Brillouin zone and high symmetry points of the NaBa$_3$N phase with a hexagonal structure: $\Gamma = (0, 0, 0)$, $M = (1/2, 0, 0)$, $K = (1/3, 1/3, 0)$, $A = (0, 0, 1/2)$, $L = (1/2, 0, 1/2)$, and $H = (1/3, 1/3, 1/2)$. (b) Band structure of the Na$_5$Ba$_3$N phase from the lowest energy bands to the valence bands near the Fermi level ε_F (straight solid line). Shown as inset is the Brillouin zone and high symmetry points of the Na$_5$Ba$_3$N phase with a simple orthorhombic structure: $\Gamma = (0, 0, 0)$, $X = (1/2, 0, 0)$, $Y = (0, 1/2, 0)$, $Z = (0, 0, 1/2)$, $S = (1/2, 1/2, 0)$, $U = (1/2, 0, 1/2)$, $R = (1/2, 1/2, 1/2)$, and $T = (0, 1/2, 1/2)$. (c) Band structure of the Na$_{16}$Ba$_6$N phase from the lowest energy bands to the valence bands near the Fermi level ε_F (straight solid line). Shown as inset is the Brillouin zone and high symmetry points of the Na$_{16}$Ba$_6$N phase with a simple cubic structure: $\Gamma = (0, 0, 0)$, $X = (0, 1/2, 0)$, $M = (1/2, 1/2, 0)$, and $R = (1/2, 1/2, 1/2)$. X is labeled at the k$_y$ direction for clarity. The k$_y$ and k$_x$ directions are completely equivalent.

four different sodium atoms gives a similar charge as compared to the sodium charge in $NaBa_3N$. Therefore similar "formal" charges are found in the interstitial metallic matrix ("sea" of sodium atoms) for the $NaBa_3N$ and Na_5Ba_3N phases. In the cubic phase $Na_{16}Ba_6N$, one of the sodium charges is practically null and the other is similar to that found in the $Na(1)$–$Na(3)$ atoms of Na_5Ba_3N. In the Na_5Ba_3N phase, one of the sodium atoms has also practically null charge, as in $Na_{16}Ba_6N$. Turning now to barium, all phases present positively charged barium atoms, with similar charges. The average barium charge and barium charge in Na_5Ba_3N and $NaBa_3N$, respectively, is similar. In the cubic phase, the barium charge is slightly more neutral. As regards to the nitrogen atoms, we interestingly see similar charges for the $NaBa_3N$ and Na_5Ba_3N phases, a clear indication that the electronic structure inside the infinite $^1_\infty[NBa_{6/2}]$ strands is similar. In the $Na_{16}Ba_6N$ phase, the negative charge on nitrogen is twice as large as compared to the other phases, mainly due to the confinement of the negative charge on the nitrogen atoms, as opposed to the $NaBa_3N$ and Na_5Ba_3N phases, where excess anionic charge on nitrogens can delocalize along the infinite strands.

As regards to the bond analysis in these nitrides, Table 2 shows Ba–N atomic distances and Mulliken overlap populations. The Ba–N distances are very similar in all three phases with similar overlap populations, a clear indication that the bonding, if any, is similar. Here we should emphasize again the coordination of the nitrogen atom with six barium atoms in perfect octahedra (face-sharing octahedra in $NaBa_3N$—see Fig. 1b—and isolated octahedra in $Na_{16}Ba_6N$—see Fig. 3) and slightly distorted octahedra (also face-sharing in Na_5Ba_3N).

Turning now to the Na–Na, Na–Ba and Ba–Ba contacts in the three phases, Fig. 6 shows a plot of overlap populations (P) versus distances (R) for several of each of the three former pairs. The two big crosses in Fig. 6 indicate the (R,P) point in metallic sodium and metallic barium, respectively. These points correspond to the overlap populations of the shortest atom–atom distance in the metals (3.658 and 4.347 Å for sodium and barium, respectively).

Let us begin with the Na–Na contacts. Fig. 6 shows that the Na–Na overlap population in the $NaBa_3N$ phase is null. This is due to the long Na–Na distance (5.995 Å). Therefore we should not expect Na–Na metallic bonds in this phase. On the other hand, large Na–Na overlap populations—as compared to metallic sodium—are found in the phases with more sodium atoms in the metallic matrix: Na_5Ba_3N and $Na_{16}Ba_6N$. While in the Na_5Ba_3N phase these populations are spread over a range of $0.023|e| \leqslant P \leqslant 0.064|e|$ and distances $3.387\,\text{Å} \leqslant R \leqslant 4.189\,\text{Å}$, very similar distances and populations are found in the cubic $Na_{16}Ba_6N$ phase. Here we should emphasize that while the shortest

Table 2
Ba–N atomic distances R(Å) and Mulliken overlap populations $P(|e|)$ in the phases $NaBa_3N$, Na_5Ba_3N, and $Na_{16}Ba_6N$

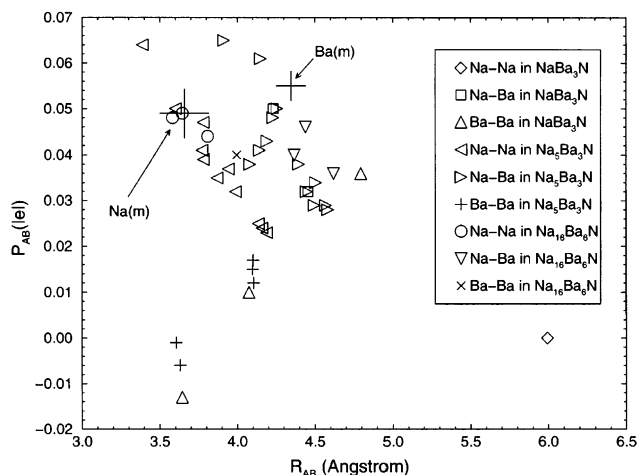|	$NaBa_3N$		Na_5Ba_3N		$Na_{16}Ba_6N$	
	R	P	R	P	R	P
Ba–N	2.734	0.156	2.729	0.159	2.825	0.153
Ba–N	—	—	2.734	0.157	—	—
Ba–N	—	—	2.746	0.150	—	—

Fig. 6. Na–Na, Na–Ba, and Ba–Ba overlap populations (P_{AB}) versus atomic distances (R_{AB}) in the three subnitrides $NaBa_3N$, Na_5Ba_3N, and $Na_{16}Ba_6N$. The big crosses indicate the (R_{AB},P_{AB}) point in metallic sodium and metallic barium (shortest R_{AB} in both metals).

Na–Na distance in $NaBa_3N$ is larger than in metallic sodium, the opposite is true for the other two phases: 3.387 and 3.581 Å for Na_5Ba_3N and $Na_{16}Ba_6N$, respectively. These values imply similar and even higher overlap populations than in the metal, as shown in Fig. 6 (note that even the larger populations, we should not expect Na–Na bonds in these phases since the bond distance in gas-phase Na_2 is 3.0789 Å and the Na–Na shortest distances in metallic Na and the nitride phases studied in this work are 3.658 and ~3.4 Å, respectively).

Turning now to the Ba–Ba contacts, we find a similar situation in all three phases, i.e., the shortest Ba–Ba distances are shorter than in metallic barium: 3.644, 3.605 and 3.995 Å in $NaBa_3N$, Na_5Ba_3N and $Na_{16}Ba_6N$, respectively. However, the Ba–Ba overlap populations are not similar to the overlap population in the metal. In the $NaBa_3N$ phase the Ba–Ba overlap populations and distances are spread over a large range of $0.04|e|$ and more than 1 Å, respectively. An analogous situation (to a less extent) takes place in Na_5Ba_3N, with a range of variation of about $0.25|e|$ and 0.5 Å for the populations and distances, respectively. As regards to the $Na_{16}Ba_6N$ phase, the single Ba–Ba overlap population is the largest as compared to the other phases ($0.040|e|$), but still smaller than in metallic barium. Therefore we find a

counterintuitive tendency as regards to the Ba–Ba contacts: larger Ba–Ba distances provide larger overlap populations for the $NaBa_3N$ and Na_5Ba_3N phases.

As regards to the Na–Ba contacts, Fig. 6 depicts the following features: The $NaBa_3N$ phase provides similar distances as compared to metallic barium and similar populations as compared to metallic sodium. The Na–Ba distances in the analogous Na_5Ba_3N phase are larger than in metallic sodium and barium and the overlap populations are spread over a range from smaller to larger populations as compared to metallic sodium and barium. Finally, in $Na_{16}Ba_6N$, the Na–Ba distances are a bit larger than in metallic barium, and the overlap populations smaller than in metallic sodium and barium.

4. Conclusions

In accord with previously proposed [3–6] bonding for $NaBa_3N$, Na_5Ba_3N, and $Na_{16}Ba_6N$, our first-principles results show that these phases feature metallic and heteropolar regions. The metallic region consists of sodium atoms separating infinite $^1_\infty[NBa_{6/2}]$ strands in the $NaBa_3N$ and Na_5Ba_3N phases and isolated $[NBa_6]$ octahedra in the $Na_{16}Ba_6N$ phase. The origin of the metallic character in these compounds can be found in the Na–Ba contacts. Even though Röhr and Simon propose Ba–N ionic bonding along the $^1_\infty[NBa_{6/2}]$ infinite strands and within $[NBa_6]$ octahedra, partial covalent character in the Ba–N bond is found according to Ba–N overlap populations and contour maps of the difference between total electron densities and superposition of atomic densities. Other interesting subnitrides, such as the larger $Ag_{16}Ca_6N_6$ (isotypic with the cubic phase $Na_{16}Ba_6N$) and $Na_{14}Ba_{14}CaN_6$, the latter described by Simon as a *nanodispersion of a salt in a metal*, are good candidates for the study of the bonding between nitrogen(nitride) and alkaline/alkaline-earth metal atoms within the interesting field of nitride and subnitride chemistry.

References

[1] D.H. Gregory, Coord. Chem. Rev. 215 (2001) 301.
[2] M.G. Burt, V. Heine, J. Phys. C 11 (1978) 961.
[3] Röhr, Angew. Chem. Int. Ed. Engl. 35 (1996) 1199.
[4] P.E. Rauch, A. Simon, Angew. Chem. Int. Ed. Engl. 31 (11) (1992) 1519.
[5] G.F. Snyder, A. Simon, J. Am. Chem. Soc. 117 (7) (1995) 1996.
[6] G.F. Snyder, A. Simon, Angew. Chem. Int. Ed. Engl. 33 (6) (1994) 689.
[7] A. Simon, Struct. Bonding (Berlin) 36 (1979) 81.
[8] U. Steinbrenner, A. Simon, Angew. Chem. 108 (1996) 595.
[9] Angew. Chem. Int. Ed. Engl. 35 (1996) 552.
[10] E. Artacho, D. Sánchez-Portal, P. Ordejón, A. García, J.M. Soler, Phys. Status Solidi (b) 215 (1999) 809.
[11] P. Hohenberg, W. Kohn, Phys. Rev. 136 (1964) 864.
[12] W. Kohn, L.J. Sham, Phys. Rev. 140 (1965) 1133.
[13] J.P. Perdew, K. Burke, M. Ernzerhof, Phys. Rev. Lett. 77 (1996) 3865.
[14] N. Troullier, J.L. Martins, Phys. Rev. B 43 (1991) 1993.
[15] L. Kleinman, D.M. Bylander, Phys. Rev. Lett. 48 (1982) 1425.
[16] S.G. Louie, S. Froyen, M.L. Cohen, Phys. Rev. B 26 (1982) 1738.
[17] S. Huzinaga, et al., Gaussian Basis Sets for Molecular Calculations, Elsevier Science, Amsterdam, 1984.
[18] R. Poirier, R. Kari, R. Csizmadia, Handbook of Gaussian Basis Sets, Elsevier Science, Amsterdam, 1985.
[19] The $Na_{16}Ba_6N$ and $Ag_{16}Ca_6N$ phases are isotypical, see Ref. [6] above. The crystal structure of the $Ag_{16}Ca_6N$ phase consists of body-cubic discrete $[NCa_6]$ octahedra surrounded by a "sea" of silver atoms.
[20] L.D. Calvert, C. Rand, Acta Crystallogr. 17 (1964) 1175.